Eng. & Tech. Journal, Vol.28, No.1, 2010

The Collision Model Between A Single Particle And A Spherical Cap Bubble In A Water Medium

Dr. Amer A. Abdul Rahman*

Received on: 27/ 5 / 2009
Accepted on: 1/10/2009

Abstract

A mechanistic model is developed to account for the collision between a single particle and a single bubble in a liquid medium. Based on the model, two penetration criteria are established under which the particle is predicted to penetrate through the bubble if any of the two criteria is satisfied. It is shown that the particle penetration is only a necessary, but not sufficient, condition for bubble disintegration in the case of single particle-single bubble collision. The penetrated bubble is shown to deform into a doughnut shape and the subsequent bubble breakage is made through the necking mechanism of the doughnut-shape bubble. Bubble disintegration occurs only if the penetrating particle has a diameter greater than the height of the doughnut-shape bubble. The column is constructed of Plexiglas with an internal diameter 10 cm and a height of 180 cm. Experiments are also performed for single particle-single bubble collision in water, using three different particles (2 mm, 3 mm glass beads and 3*3 mm PVC cylinder) with Reynolds no. and Weber no. are (953, 1512 and 840) and (5.68, 9.45 and 5) respectively . Two markedly different collision phenomena are observed. A small and/or light particle is unable to penetrate through the bubble and is ejected after collision. A medium particle can penetrate through the bubble but may not break the bubble. The two phenomena are all well predicted by the proposed model.

Keywords: three phase fluidized beds, and bubble breakage.

نموذج اصطدام بين جسيم صلب منفرد مع فقاعة منفردة من نوع القبعة في وسط مائي

الخلاصة

صمم موديل ميكانيكي للاصطدام ما بين جسيم صلب منفرد وفقاعة منفردة في وسط سائل. واعتماداً على هذا الموديل اعتمد سلوكان للاختراق من خلالها يتوقع للجسيم ان يخترق الفقاعة اذا روعيت هذه السلوكيات. لقد بُيّن ان اختراق الجسيم ضروري ولكن ليس كافياً كشرط لتحلل فقاعة في حالة اصطدام جسيم فقاعة منفردة. ان الفقاعة المخترقة قد بُيّنت انها ستشوه الى شكل فطيرة دونت والتكسر التالي للفقاعة ينتج من خلال ميكانيكية العناق المختصة بشكل الدونت. وتحلل الفقاعة لا يحصل الا اذا كان الجسيم الثاقب له قطر اكبر من ارتفاع الفقاعة ذو الشكل الدونت. تم اجراء التجارب باستخدام عمود مصنوع من مادة بليكسيكلاس وبقطر داخلي 10 سم وبطول 180 سم. وأجريت التجارب ايضاً لتصادم جسيم منفرد مع فقاعة منفردة في الماء بأستخدام ثلاث جسيمات مختلفة تتعلق بالتصادم (2 , 3 ملم حبيبات زجاجية و 3*3 ملم من مادة البولي فنيل كلورايد) مع رقم رينولدز ورقم ويبر (953, 1512, 840) و (5.68 , 9.45 , 5) بالترتيب. ولوحظت ظاهرتان مختلفتان للتصادم, ان جسيم صغير و/او خفيف يكون غير قادر على اختراق الفقاعة ويقذف بعد التصادم. وجسيم

*Chemical Engineering Department, University of Technology/ Baghdad

https://doi.org/10.30684/etj.28.1.1
2412-0758/University of Technology-Iraq, Baghdad, Iraq

متوسط يستطيع اختراق الفقاعة ولكن قد لا يكسرها.. وكل هذه الظواهر كانت متوقعة للموديل المقترح.

1. Introduction

In order to predict the bubble size distribution, it is essential to understand the mechanisms underlying these processes.

The two competing processes on bubble coalescence and disintegration ultimately determine the equilibrium bubble size distribution in the system (Ostergaard, 1966).

In a (gas-liquid-solid) fluidized bed, the bubble size is a key factor affecting the hydrodynamics and the overall gas-liquid mass transfer rate. As bubbles a scent from the gas distributor, they may undergo coalescence and disintegration by several mechanisms (Muroyama and Fan, 1985).

When small particles are present in a gas-liquid system, it was observed (Ostergaard, 1966) that bubble coalescence is enhanced and the bubble size increases rapidly above the gas distributor.

Bubbles in a such system one quite uniform and relatively small in size compared to those observed in a solid-free gas-liquid system (Ostergaard, 1969; Lee et al., 1974; Bruce and Revel-Chion, 1974; Muroyama and Fan, 1985).

Thus, the presence of large particles in a gas-liquid system tends to yield the dispersed bubble flow regime, whereas the presence of small particles yields the coalesced bubble flow regime.

Epstein (1981) indicated that the particle size corresponding to the flow regime transition is around 3 mm for an air-water-glass sphere system. Mastuura and fan (1984), however, indicated that in addition to the particle size, particle density and gas and liquid velocities may affect the flow regime transition as well.

The bubble was assumed to disintegrate when the particle with adequate inertia induces a hemispherical indentation on the bubble roof. Their theory leads to the criterion of a critical Weber number, $W_e = (\rho_s u_b^2 d_p / \delta)$, of three beyond which the bubble will break. The results of particle penetration without bubble breakage were also reported by Frijlink (1987) Henriksen and Ostergaard (1974) thus attributed bubble disintegration to a completely different mechanism of Rayleigh-Taylor instability on the roof of the bubble.

Bubble properties such as size, rising velocity and frequency have been measured and investigated in a three-phase fluidized beds with viscous medium by Son, Kang and Kim (2007). It has been found that the size and frequency of bubbles have increased with increasing gas or liquid velocity. The bubble size and rising velocity have increased but the frequency decreased, with increasing liquid viscosity.

Bubble behavior, including bubble Sauter diameter, bubble rise velocity, bubble frequency and local gas holdup in different radial and axial position, was measured using a dual electro-conductivity prob in air-water-glass beads fluidization systems by Chen et al. (1998). It has

been found that the bubble characteristics differ significantly in various flow regimes, depending on the operating conditions, the radial distribution of bubble parameters also changes from one flow regime to another.

Barghi et al. (2001) studied fluidization regimes in liquid-solid and gas-liquid-solid fluidized beds. The liquid velocities at which regime transition occurs in liquid-solid and gas-liquid-solid systems were obtained for mono size and multi component systems. Minimum fluidization, complete fluidization and complete mixing velocities of particles were obtained from pressure drop measurements, a collision technique or a conductivity method.

The effect of pressure and surfactants on the phase holdups and flow regime transition velocities of gas-liquid-solid fluidized beds were investigated by Rudkevitch and Macchi (2008). The effect of pressure on the bed phase holdups is significant and more pronounced at larger gas flow rates where pressure has a greater effect on the equilibrium bubble size. The addition of a surfactant leads to an increase in the gas holdup and a lowering of the solids and liquid holdups. The presence of a surfactant with a liquid flow results in shearing of the bubbles across the gas-liquid distributor, limiting the effect of pressure.

The mechanism proposed by Henriksen and Ostergaard also has flows. Based on their mechanism bubble breakup in an air-water-glass sphere system can occur only if the particle diameter exceeds 8.5 mm, while bubble breakup in the same system was experimentally observed to occur with 2.5 mm particles (kim et al., 1977).

Chen and Fan (1988) indicated that Bellman and Pennington's theory (1954) was originally developed for a plane surface with a two-dimensional sinusoidal disturbance. A real bubble is neither flat on the roof nor is the disturbance by a particle two-dimensional. Most importantly, when a particle collides with a bubble, the particle does not leave the bubble interface immediately. Thus, the bubble breakup by particle collision is more likely due to the collision itself rather than the Ray Leigh-Taylor instability induced by the collision.

Daw and Halow (2000) was identify multivariate dynamic characteristics in the pressure signals that can be correlated with specific physical phenomena in the bed, including spatial distribution of bubbles, characteristic bubble size, bubble velocity, and global bed oscillations.

In the present study, a more through mechanistic model is developed to account for the collision of a single particle with a single bubble. Based on this model, criteria for particle penetration and the sub sequent conditions for bubble breakup one established.

Experimental observations of the collision between a single spherical cap bubble and particle, with various sizes and densities.

Analysis

In the following analysis, the process of the collision between a single particle and a single bubble is subdivided into their sequences of periods: prior to collision, during collision and after collision. The particle penetration conditions are

established during the collision period and the subsequent conditions for bubble breakup are discussed.

Prior to collision

Although the viscous force is negligible compared to the inertia force for the case of a large and heavy particle colliding with a large bubble. It could be the dominant force to the case of a small particle. This is elucidated in Fig. (1), in which the particle approaches a bubble, head to head, in an infinitely extended liquid medium.

The descending particle has its front stagnant point facing downward while the bubble has its stagnant point facing upward, as symbolized by positive signs in Fig. (1), indicating that the stagnant point has a higher pressure than other locations at the same level. The layer in front of the stagnant point, depioted by the excess line, indicates the effective range of the excess pressure, i.e. the boundary layer.

Because of the approaching of the two excess pressure layers, the particle and the bubble tend to divert from the center line and to avoid collision as much as possible.

The degree of the diversion depends on the Reynolds number and the total mass of the particle. The greater the Reynolds number, the thinner the boundary layer is and the faster the approaching velocity become.

Combination of these two effects of a greater Reynolds number yield a shorter response time for avoiding collision. The total mass is also affecting the system in a similar manner as that of the Reynolds number. The greater the total mass is the more difficult it becomes to avoid collision because of greater inertia.

In the present experimental, the smallest particle employed is a 2 mm glass sphere. Under this condition, the viscous force involved in the period prior to collision is assumed to be negligible in the following analysis (Kim et al., 1977).

The collision process

Fig. (2) Shows the system diagram of a single particle with a diameter of dp penetrating into a bubble at a depth of h. A bubble of a spherical cap shape is considered, having the dimensions of width b, height H and radius of curvature R, and rising at velocity of U_b.

Prior to the contact of the particle, the gas pressure within the bubble is greater than that of the liquid adjacent to the bubble roof, given by the Young-Laplace equation (Daizo et al., 1983):

$$\Delta P = \frac{2d}{R} \qquad \ldots\ldots (1)$$

Now, consider the forces acting on the penetrating particle at a depth h. The particle is subject to a net upward face, F, the summation of four different for as, which results in an upward acceleration a, as expressed by (Daizo et al., 1991):

$$F = \pi/6\, d_p^3\, \rho_l\, g - \pi/6\, d_p^3\, \rho_s\, g + \delta\, \pi\, d_p - (2\delta/R - \rho_l hg)\, \pi/4\, d_p^2.$$

$$= \pi/6\, d_p^3\, \rho_s\, a. \qquad \ldots\ldots..(2)$$

The first and second terms on the right-hand side of Eq. (2) are the buoyant force and the gravitational force respectively. The third term is the surface tension force and the fourth term is the pressure term, which is the liquid head due to penetration corrected by the initial pressure difference according to Eq.(1).

In the development of the force balance of Eq. (2) several assumptions are made. It is assumed

that the particle is wetted at all time during the penetrating process, and the particle is not indirect contact with the gas bubble. This assumption is valid for wetting particles which are most commonly encountered in three-phase fluidized bed operation. It is also assumed that the contact surface between the bubble and the particle maintains hemispherical during the collision, which is probably true when the contact time is short and the penetrating particle creates a hole of about the same size of the particle itself.

The total mass of the particle in Eq.(2) is taken to be the mass of the particle alone, which implies that the added mass of the particle is assumed to be insignificant during collision.

Considering the fact that when the particle is immersed in a bubble as depicted in Fig.2, the particle is no longer surrounded by a relatively upward liquid flow and these is no associated wake formation behind the moving particle.

In addition, the fluid affected by the particle motion is confined to the limited portion of the liquid hole directly behind the particle. The viscous drag in Eq. (2) is ignored due to the same reason that the particle is not surrounded by a relatively upward liquid flow.

By using the condition of zero penetration depth at the initial contact:

t = o, h = o ….. (3)

The initial value of particle acceleration can be obtained combining Eqs. (2) and (3) yielding

$$a_o = g\frac{r_l - r_s}{r_s} - \frac{6d(1+dp/2R)}{r_s dp^2} \quad \ldots.(4)$$

Since initially the bubble is ascending and the particle is descending, the only possibility that the particle does not penetrate through the bubble is that the particle accelerated upward to catch up with the ascending bubble.

From Eq. (2), it is noted that the acceleration, a, is a monotonic decreasing function of penetration depth h. Hence, if the initial acceleration a_o, is negative, the acceleration is always down ward and the particle always penetrates through the bubble.

This leads to the first criterion for particle penetration:

$a_o < o$ …… (5)

$$\frac{dp^2(r_s - r_l)g}{d(1+dp/2R)} > 6 \quad \ldots.. (6)$$

By differentiating Eq. (2) twice and elimination the variable of h using the relation of d^2h/dt^2 equal to – a, the differential equation expressed in terms of the variable "a" alone:

$$\frac{da^2}{dt^2} - w^2 a = o \quad \ldots. (7)$$

Where

$$w = \left(\frac{3r_L g}{2r_s dp}\right)^{1/2} \quad \ldots\ldots. (8)$$

The two initial conditions for Eq.(7) the:

t = o, $a = a_o$ …… (9)

And

$$t = o, \frac{d_a}{d_t} = -w^2(\mathbf{U}_b + \mathbf{U}_{po}) \quad \ldots.. (10)$$

The second initial condition is obtained by differentiating Eq. (2) once and dh/dt being the initial approaching velocity between the particle and the bubble. With Eqs. (9) and (10), the acceleration of the particle can be solved to yield.

$a = a_0$ cash $(\omega\tau) - \omega(U_b + U_{po})$ sinh (wt) … (11)

and the particle ascending velocity can be obtained by integrating Eq. (11) to yield.

$$U_p = U_{po} + \frac{a_o}{w}\sinh(wt) - (U_b + U_{po})[\cosh(wt) - 1] \quad \ldots. (12)$$

In obtaining Eq. (12), it is assumed that the virtual mass of the bubble is much greater than the mass of the particle so that the bubble ascending velocity is not affected by collision.

In order for the particle being caught by the bubble, the particle has to be accelerated upwards to the same velocity of the bubble. From Eq.(12), the time required to accelerate the particle to the ascending velocity of u_b becomes

$$\tanh(\omega\tau) = (u_b + u_{po})\ \omega/a_o \quad \ldots. (13)$$

If Eq. (13) is greater than one, t has no real solution. This implies that is impossible to accelerate the particle to the ascending velocity of the bubble and the particle always penetrates through the bubble.

Thus, the second criterion of particle penetration becomes

$$\frac{U_b + U_{po} w}{a_o} > 1 \quad \ldots\ldots. (14)$$

Physically, the condition of eq. (14) can be met when the particle inertia is sufficient to permit particle penetrating an adequate depth into the bubble such that the liquid head behind the particle becomes dominant and then after, particle penetration becomes automatic.

The particle penetration depth, h, can be estimated by integrating Eq.(12) to yield:

$$h = \frac{U_b + U_{po}}{w}\sinh(wt) - \frac{a_o}{w^2}[\cosh(wt) - 1] \ldots (15)$$

In order for the particle not to penetrate through, the particle has to be accelerated fast enough to the ascending velocity U_b before penetrating the whole depth of the bubble, H. This leads to the third criterion of particle penetration. By combining Eqs.(13) and (15), the penetration depth of the particle at time τ is given by:

$$h_p = \frac{(U_b + U_{po})}{w}\sinh(wt) - \frac{a_o}{w^2}[\cosh(wt) - 1]$$

$$= \frac{a_o - \left[a_o^2 - (U_b + U_{po})^2 w^2\right]^{1/2}}{w^2} \ldots\ldots\ldots (16)$$

And the third penetration condition requires that: $h_p > H$ ……. (17)

Thus, the particle will penetrate through the bubble if any one of the three conditions, Eqs. (6), (14) and (17), is satisfied.

It is important to note that the three criteria should be tested in accordance with the sequence presented here.

Consequence after collision

There are two situations that could possibly occur after collision. If a particle is small and/or light such that non of the three penetration conditions are satisfied, the particle is unable to penetrate through the bubble and is ejected after collision. Its ultimate penetration depth can be estimated by Eq. (16). The duration of the collision process, from the point when the particle and the bubble contact to when the particle being ejected, can also be estimated. By setting h = o in Eq. (15), the colliding duration time, τ_c, satisfies the following equation:

$$\frac{U_b + U_{po}}{w}\sinh(wt_c) - \frac{a_o}{w^2}[\cosh(wt_c) - 1] = o \ldots. (18)$$

Notice that Eq. (18) may have more than one solution and τ_c = o automatically satisfies the equation. This particular solution is the initial contact time and should not be regarded as the solution of the duration time.

If, on the other hand, the particle is large and/or heavy enough such that at least one of the three penetration criteria is satisfied, the particle penetrates through the bubble. The bubble being penetrated is assumed to deform into a doughnut shape, as depicted in Fig.3. The diameter of the center hole of the doughnut-shape bubble is taken to be that of the penetrating particle. The height of the doughnut shape bubble, H_d, can be estimated by requiring that the deformed bubble has the same volume as the original under formed bubble:

$$\frac{1}{4}\Pi^2 H_d^2\left(H_d + d_p\right) = \frac{1}{3}\Pi H^2(3R - H) \quad \ldots(19)$$

Note that Eq. (19) has only one real solution for H_d. The doughnut-shape bubble only exists momentarily; the presence of surface tension tends to reduce the interfacial area of the bubble will red form accordingly.

There are two different ways that the surface tension can reduce the interfacial area. Note that the center hole of the doughnut-shape bubble in Fig.(3) has two radii of the curvature of opposite signs, where R_1 swings in the plane of the paper and R_2 swings in the right angle to it.

If R, is greater than R_2, the net surface tension is acting in the direction of shrinking R_2. Thus, if the particle diameter is less than the height of the deformed bubble, it yields

$$d_p < H_d \quad \ldots. (20)$$

And the center hole of the doughnut-shape bubble will shrink, and the doughnut-shape bubble tends to recover to its original shape. In such a case, particle penetration does not result in bubble disintegration. If, on the other hand, R_2 is larger than R_1, it yields:

$$d_p > H_d \quad \ldots.. (21)$$

And the net surface tension is acting in the other direction of shrinking process. Boys (1890) indicated that a uniform cylindrical bubble possesses a critical length equal to the circumference of a cylindrical bubble beyond which it is unstable toward necking. Note that the shortest length of the doughnut bubble, Πd_p, exceeds the circumferences, ΠH_d, when Eq. (21) is satisfied.

The preceding mechanism concludes that particle penetration may not necessarily result in bubble disintegration. The bubble will break only if the penetrating particle has a diameter greater than the height of the doughnut-shape bubble.

Experimental

The experimental apparatus for the visualization studies of the dynamic behavior of a single particle and a single bubble collision is shown schematically in Fig.4. The column is constructed of Plexiglas with an internal diameter 10 cm and a height of 180 cm.

In order to eliminate the optical distortion by the cylindrical column, the test section of the column is enclosed in a square viewing vessel made of Plexiglas and filled with water. Although the apparatus is equipped with a liquid circulation system, only stationary water is used.

A single gas bubble is generated from stainless steel nozzle of 0.6 cm outside diameter located at the centre of the column bottom using a solenoid valve. The particle is dropped manually from the top through a guiding tube located at the center of the column.

Digital camera type (OLYMPUS, C-400/ZOOM) with high resolution (4 pixels) was used in the experimental work. This camera is synchronized with the solenoid value and the ascending velocity of the video camera is adjusted to that of the rising bubble so that the bubble appears to be stationary on the monitor through the collision process.

Three different particles are used in the experiments and their physical properties are given in Table 1.

The liquid and the gas employed are tap water and nitrogen respectively.

In all experiments, the bubble size is controlled in the range of a spherical cap bubble for several reasons.

First, a large spherical cap bubble is adopted to be consistent with the assumption of the bubble virtual mass being greater than the particle mass in the analysis. In addition a spherical cap bubble rises more steadily in the liquid which is essential to the occurrence of head-on collision with the descending particle, (Kim et al., 1977).

The use of a spherical cap bubble also has the merit of avoiding the complication due to the contamination of tap water.

The surface tension at the bubble roof, particularly for the portion around the front stagnant point, can be taken as that of pure water because the contamination on the bubble roof is continuously carried a way to the rear of the bubble by the sweeping liquid flow.

Results and Discussion

In Figs.5-6, two different phenomena of single particle-single bubble collision are depicted by two series of photographs reproduced from the video recorder. The photographs appear to consist of a number of horizontal lines, which are caused by reproduction and enlargement of pictures from a TV screen. In each photograph only one field, consisting of either an odd or an even number of lines, of the screen is shown.

Figure 5 (a-g) shows a series of photographs of a 2 mm glass sphere colliding with a spherical-cap bubble, which represents the collision of a small and/or light particle with the bubble.

The time interval between two consecutive photographs is one-sixtieth of a second.

In Fig 5 (a), the particle with its path shown by a shadow on the photo, approaches the bubble almost vertically, the particle appears as a shadow due to two reasons. First, the relative velocity between the particle and the bubble is high and the particle and the particle travels an appreciable distance during the time interval when one field of screen is taken (one-sixtieth of a second), where the Reynolds no and Weber no. are 953 and 5.68 respectively.

Second, due to the characteristics of the video camera the ghost of the previous image is superimposed onto the present image. The arrow on the photo indicates the location of the particle. In Fig. 5 (b), as the particle closes in for collision, it is slightly deflected to the left due to the viscous effect discussed in the beginning of the analysis. In Fig. 5 (c), the particle collides with the bubble, with the tail of the ghost of the particle path line still shown by a diffused line.

In Fig. 5 (d) and (e), the particle merges into the bubble and completely disappears. In Fig. 5 (f) and (g), the particle is unable to penetrate through and is ejected to the left of the bubble. The duration time

of collision can be estimated by counting from Fig. 5 (c) to Fig. 5 (f) which is about one-twentieth of a second.

Very similar collision phenomena of no particle penetration and particle ejection after collision were also observed when using the 3 mm *3mm cylindrical PVC particle. The colliding duration time for the PVC particle was estimated to be about one fifteenth of a second.

Figure 6 (a-d) shows the collision of a 3 mm glass sphere with the bubble, representing the phenomenon for the collision of a medium particle. In Fig.6 (b) and (c), the penetration of the particle is clearly depicted, showing a funnel shaped hole in the bubble.

In Fig. 6 (d), after the particle penetration, the funnel-shaped hole in the bubble start to merge from the bubble base and the penetrated bubble eventually recovers to its original shape. The particle is able to penetrate through but is unable to break the bubble.

Note that the particle path line in Fig. 6 (b) is deflected only very slightly by the bubble, compared to that in Fig. 5 (b). This is due to the fact that the 3 mm particle has a greater mass and Reynolds number which is equal to 1512.

Comparison of the theoretical predictions and the experimental results are given in Table 2. The results of the present experiments using three different particles with three different collision phenomena are all very well predicted by the present criteria with co-efficient 0.994. A maximum of 3.5% deviations was found.

The phenomena of bubble deformation and the consequent bubble breakage exactly follow the proposed mechanisms. The penetrated bubble indeed deforms into a doughnut shape.

The recovery of the doughnut-shape bubble is by the mechanism of merging the center hole and the breakup of the doughnut-shape bubble is by the mechanism of necking. Note that not only can the present criteria predict the qualitative behavior of the particle collision; they can also predict it quantitatively. For instant, the criteria predict that a 2 mm glass sphere cannot penetrate through the bubble while a 3-mm glass sphere can. Quantitative comparison of the colliding duration time is give in the following.

Based on Eq. (15) the penetration depth, h, as function of time for the 2 mm glass sphere and d_b = 2.27 cm is plotted in Fig. 7. The maximum penetration depth, hp, calculated by Eq. (16) is shown in Fig. 7 to be less than the bubble height, H, predicting that the particle cannot penetrate through the bubble, in agreement with the present observation. Detailed comparisons with the experimental penetration depth, however, cannot be made because the glass sphere cannot be clearly traced as shown in Fig. 5 (d) and (e).

The colliding duration time, τ_c, is the point at which the penetration depth retreats to Zero, which is estimated to be 0.041 s. The experimental collision time is estimated by counting the number of video frames from the particle contact to particle ejection.

For both cases involving a 2 mm glass sphere and a 3 mm * 3 mm PVC cylinder, the colliding duration times are very precisely predicted, as

shown in Table 2. The discrepancies of the predictions are within the precision of the time measurement (one-sixtieth of a second) by the present method.

The experimental results of Henriksen and Ostergaard (1974) and those of Frijlink (1987) are also used for comparisons in Table 2. Henriksen and Ostergaard (1974) employed a different experimental technique of continuous downward liquid flow through a taped tube to hold the bubble stationary. In their experiments, a spherical cap bubble with sizes 2 cm nearly similar to those in the present experiments was used.

Concluding Remarks

Two criteria of particle penetration through a bubble are established based on the collision theory between a single particle and a single bubble. The particle is predicted to penetrate through the bubble if any one of the two penetration criteria is satisfied. It is shown that particle penetration is only a necessary, but not the sufficient condition for bubble disintegration in the case of single particle-single bubble collision.

The penetrated bubble is shown to deform into a doughnut shape and the bubble will disintegrate only if the penetrating particle has a diameter greater than the height of the doughnut-shape bubble.

Based on experimental observations, there exist two different phenomena underlying the collision between a single particle and a single bubble in a liquid medium.

1. A small and/or light particle (2 mm glass sphere and 3 mm *3 mm PVC cylinder is unable to penetrate through the bubble and is ejected after collision.
2. A medium particle (3 mm glass sphere can penetrate through the bubble but may not disintegrate the bubble.

These two different phenomena are all well predicted by the present theory.

Notations

a	upward acceleration of the particle during collision, L/T^2.
a_o	initial value of the particle acceleration, a, L/T^2.
b	bubble width, L.
d_b	Equivalent diameter of the bubble, L.
d_p	particle diameter, L.
F	net upward force acting on the particle during collision, N.
g	gravitational acceleration, L/T^2.
h	particle penetration depth, L.
h_p	the deepest penetration of the particle, L.
H	bubble height, L.
H_d	height of the doughnut-shape bubble, L.
ΔP	pressure difference between the bubble and the adjacent liquid before collision, N/L^2.
R	radius of curvature of the bubble, L.
R_1	radius of curvature of the deformed bubble, referring to Fig.3, which equals $H_d/2$, L.
R_2	radius of curvature of the deformed bubbles, referring to Fig.3, which equals $d_p/2$, L.
t	time,T.
U_b	bubble ascending velocity, L/T.
U_p	particle descending velocity, L/T.
U_{po}	initial descending velocity of the particle, L/T.

W_e weber number, $\rho_s U_b^2 d_p/\delta$

Greek letters

ρ_L liquid density, M/L^3.

ρ_s solid density , M/L^3.

δ Surface tension, N/L.

τ time required to accelerate the particle to U_b, T.

τ_c the duration time of the whole collision, T.

$Ø_s$ sphericity of the particle.

ω angular velocity defined by eq. (8), 1/T.

References

[1] Adamson, A.W., (1982), physical chemistry of surface, 4th Edition, Wiley, New York.

[2] Barghi, S. and Briens, C. L., (2001), "Fluidization Regimes in Two and Three – Phase Fluidized Beds: Comparison Between Measurement Techniques", Can. J. Chem. Eng., Vol.79, June.

[3] Bruce, P.N. and Reuel-Chion, L, (1974), Bed Porosity in three-phase fluidization. Powder Technol. 10, 243-249.

[4] Boys,C. V., 1890, Soup Bubbles and the Forces that Mould Them. Society for Promoting Christian Knowledge, London.

[5] Chen, Z., Zheng, C., Feng, Y. and Hofman. H., (1998), "A Generalized Back-Flow Model to Predict the Tracer Response in Liquid-Liquid Stagewise Contactors", Can. J. Chem. Eng., Vol.76, No. 2.

[6] Chen, Y.M. and Fan, L.S., (1988), On the Criteria of Ray Leigh-Taylor instability at a curved interface by a local force balance. Chem. Eng. Sci. (in review).

[7] Daizo, K., Ryozo, T., (1983), Proceeding of the Fourth International Conference on Fluidization.

[8 Daizo, K., Levenspiel, O., Fluidization Engineering, 2nd edition, Butter Worth-Heinemann, Stoneham, 1991.

[9] Daw, C.S., Halow, J.S., Finney, C.E.A., and Nguyen, K., (2000) "Characterizing the Hydrodynamics of Bubbling Fluidized Beds with Multivariate Pressure Measurements", 2000 AICHE Annual Meeting (Loa Angeles, California USA, November 12-17), Paper 20e.

[10] Epstein, N., (1981), Three-phase fluidization: some knowledge gaps. Can. J. Chem. Eng. 59, 649-657.

[11] Frijlink, J.J., (1987), physical aspects of gassed suspension reactors, Ph.D., dissertation, Technische Universiteit Delft, Holland, pp.23-25.

[12] Henriksen, H.K. and Ostergaard, K., (1974), on the mechanism of breakup of large bubbles in liquids and three-phase fluidized beds. Chem. Engng. Sci. 29, 626-629.

[13] Hinze, J. O., (1955), Fundamentals of the hydrodynamic mechanism of splitting in dispersion processes, A.I.Ch.E.J.1, 289-295.

[14] Kim, S.D., Baker, C.G.J. and Bergougnou, M.A., (1977), Bubble characteristics of three phase fluidized beds. Chem. Engng. Sci. 32, 1299-1308.

[15] Lee, J. C., Sherrad, A.J. and Buckley, P.S., (1974), Optimum particle size in three phase fluidized bed reactors, in Fluidization and Its Application (Edited by H. Angelino et al.),

pp. 407-416, Cepadues Editions Toulouse.

[16] Matsura, A. and Fan, L. S., (1984), Distribution of bubble properties in a gas-liquid-solid fluidized bed, A.I. Ch. E. J. 30, 894-903.

[17] Muroyama, K. and Fan, L.-S., (1985), Fundamentals of gas-liquid-solid fluidization, A.I., Ch. E. J. 31, 1-34.

[18] Ostergaard, K. (1966), On the growth of air bubbles formed at a single orifice in a water fluidized bed Chem. Engng. Sci. 21, 470-472.

[19] Ostergaard, K. (1969), Studies of gas-liquid fluidization. Danish Technical Press, Copenhagen.

[20] Rudkevitch, D., and Macchi, A., (2008) "Hydrdynamics of a High Pressure Three-Phase Fluidized Bed Subject to Foaming", Can. J. Chem. Eng., Vol.86, Issue 3, Pages (293-301).

[21] Son, M.S., Kang, S.H., Kim, Y., Kang, Y., and Kim, S.D., (2007) "Bubble Properties in Three-Phase Inverse Fluidized Beds with Viscous Liquid Medium", Chemical Engineering and Processing, Vol.46, Issue 8, Pages (736-741), August.

Table (1) Physical properties of the particles employed in the experiments

Particles	Size (mm)	Shape	Density (g/cm^3)
2mm glass beads	2	Sphere ($Ø_s$ = 1.0)	2.5
3mm glass beads	3	Sphere ($Ø_s$ = 1.0)	2.52
PVC cylinder	3*3	Cylindrical	1.47

Table (2) Comparisons of the theoretical predictions and the results from the present experiments and those from Henriksen and Ostergaard's (1974) and Frijlink's (1987) experiments.

Investigators	Particles	Bubbles	Experimental results	Predictions based On the present criteria
Present study	2mm glass sphere	b=3.58 cm H=0.91 cm d_b=2.27 cm U_b=28.6 cm/s	No particle Penetration, Particle Ejected after Collision 0.033s< τ_c < 0.05s	No particle Penetration, Particle ejected After collision τ_c=0.041s
	3mm*3mm PVC cylinder	b=3.47 cm H=0.91 cm d_b=2.22 cm U_b=28.6 cm/s	No particle Penetration, Particle Ejected after Collision 0.05s< τ_c < 0.067s	No particle Penetration, Particle ejected After collision τ_c=0.057 s
	3mm glass sphere	b=3.47 cm H=1.08 cm d_b=2.35 cm U_b=30 cm/s	Particle Penetration, No bubble breakup	Particle Penetration, No bubble breakup
Henriksen and Ostergaard (1974)	3mm glass sphere 6mm glass sphere 5mm steel sphere	d_b=2cm d_b=2cm d_b=2cm	Particle Penetration, No bubble Breakup	Particle Penetration, No bubble breakup

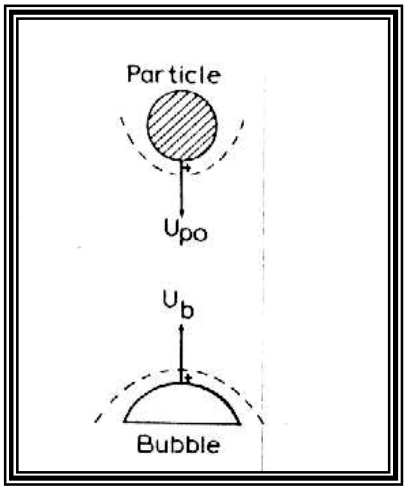

Figure (1) System configuration of a particle approaching spherical-cap bubble

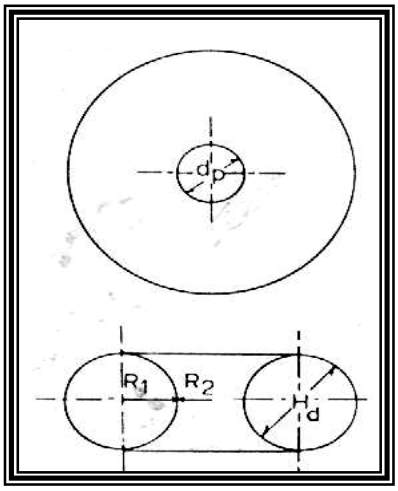

Figure (3) System configuration of a doughnut-shape bubble

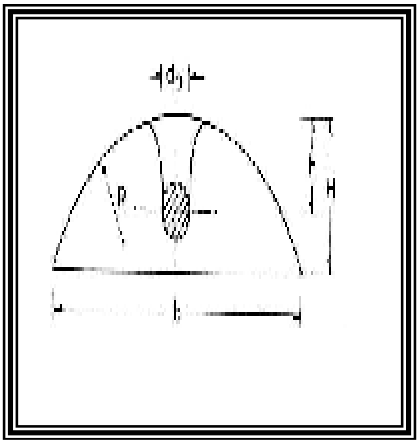

Figure (2) System configuration of a particle colliding with a spherical-cap bubble

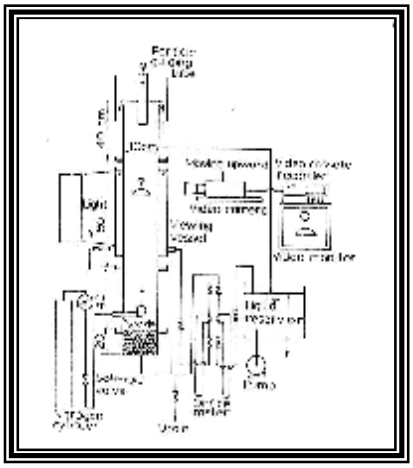

Figure (4) schematic diagram of an experimental apparatus for visual studies of single particle- single bubble collision

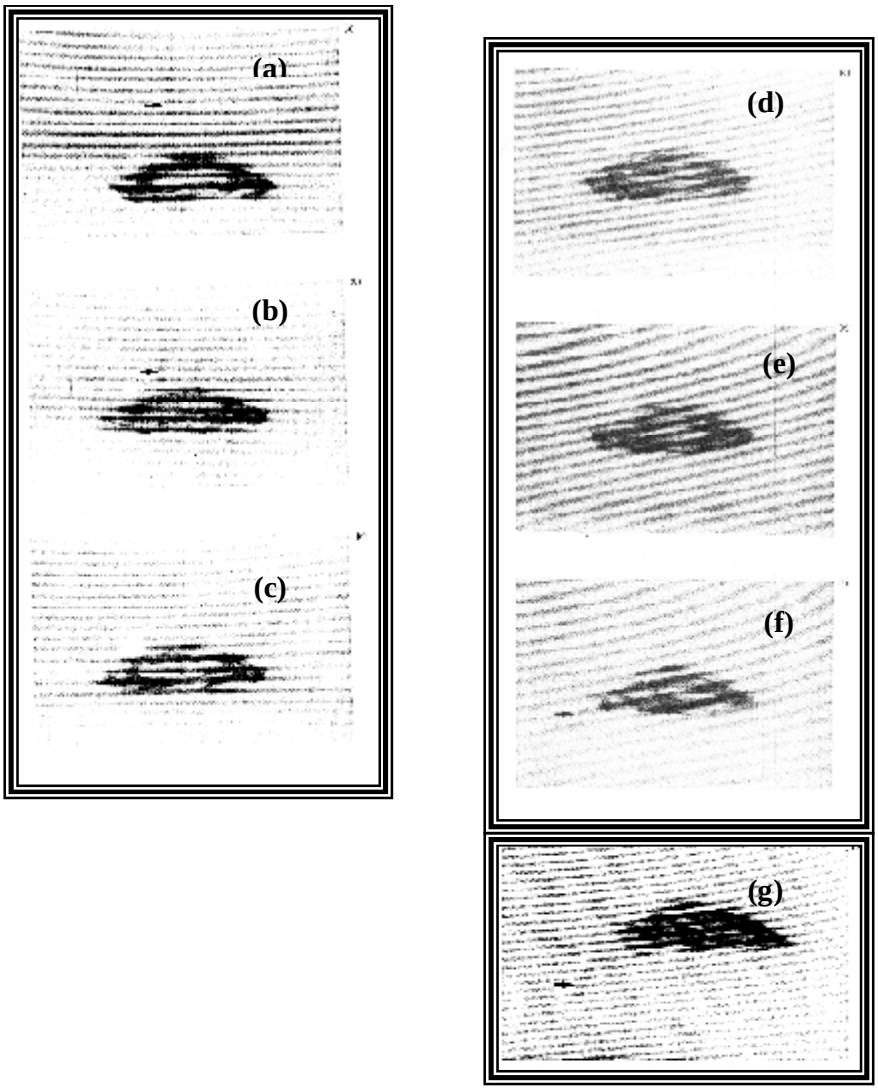

Figure (5) Collision sequence of a 2-mm glass sphere and a spherical-cap bubble (d_b =2.27 cm), taken by Digital camera type (OLYMPUS, C-400/ZOOM) with high resolution (4 pixels), the particle indicated by the arrow, does not penetrate through and ejected to the left

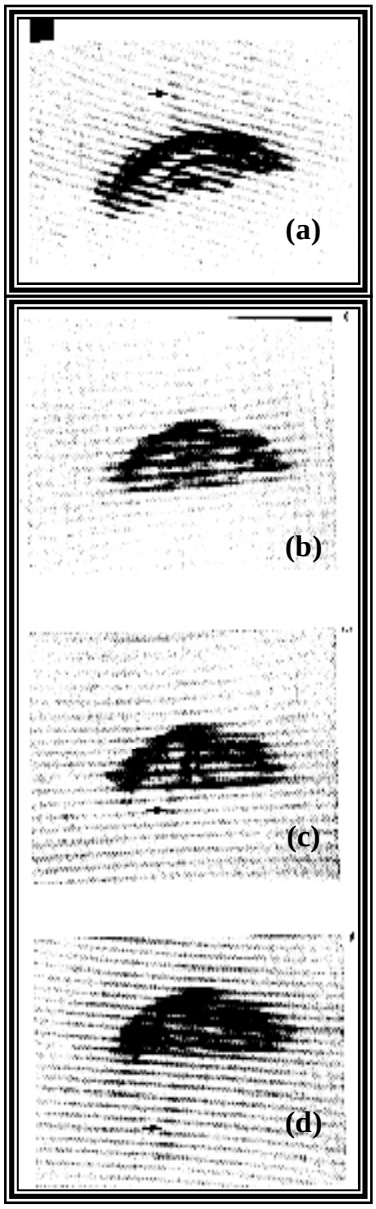

Figure (6) Collision sequence of a 3- mm glass sphere and a spherical-cap bubble (d_b =2.22 cm), the particle indicated by the arrow, penetrates through but not break the bubble

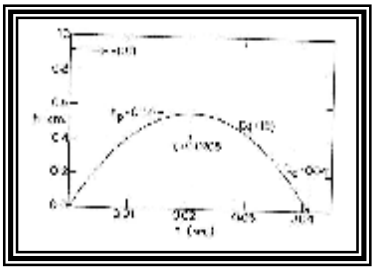

Figure (7) Prediction of the penetration depth vs. time relationship of the collision of a 2-mm glass with a bubble (b=3.58 cm, H=0.91 cm, d_b=2.27 cm)